IJRRS
International Journal of Reliability, Risk and Safety: Theory and Application

Online ISSN: 2676-3346

OPEN ACCESS

Vol. 7/ Issue 1/ 2024/ pp. 37-44
DOI: 10.22034/IJRRS.2024.7.1.5
Received: 19 January 2024, Revised: 04 March 2024, Accepted: 05 March 2024
Available online at: https://www.ijrrs.com

Short Technical Paper

# Probability assessment of photoneutron production of Varian-Clinac ix linear accelerator using Monte Carlo simulation

**Saeed Zare Ganjaroodi[1*], Mohammadreza Fathalizadeh[2] and Ehsan Zarifi[3]**

1- Department of Physics and Energy Engineering, School of Sciences, Amirkabir University of Technolog , Tehran, Iran

2- Faculty of Engineering, Science and Research Branch, Islamic Azad University, Tehran, Iran

3- Nuclear Science and Technology Research Institute (NSTRI), Tehran, Iran

* **szareganjaroodi@aut.ac.ir**

**Abstract**

Overdose in the patient's body disrupts the treatment process and may have devastating effects. On the other hand, if the particle is a neutron, this effect would be multiplied. Because neutrons in the energy range of about 0.1 to 2 MeV produced in medical linear accelerators have a Quality Factor (QA) of 20, which creates a high equivalent dose in the tissue. In this paper, the photoneutron production probability of components of the 18 MV Varian-Clinac ix linear accelerator has been performed using the Monte Carlo simulation. The contribution of each gantry component of the accelerator and phantom in neutron production per gray of photons was calculated. Results showed that the largest ratio in the production of photoneutrons belongs to the primary collimator per photon gray per square centimetre. Also, in the target, which is the first source of photon neutron production, the flux of thermal neutrons is calculated at zero.

**Keywords:** Neutron; Varian-Clinac ix; Production probability; Monte Carlo simulation.

## Nomenclature and Units

| Symbol | Parameters | Units |
|---|---|---|
| *E* | Energy | MeV |
| *E* | Energy (for the clinical system) | MV |
| $\psi$ | Fluence | (#/cm$^2$.Gy$^{-1}$) |
| *D* | Dose | (mSv.Gy$^{-1}$) |
| *MeV* | Mega electron volt | - |
| *MV* | Mega volt | - |
| *Sv* | Sivert | - |
| *Clinac* | Clinical linear accelerator | - |
| *PET* | Positron Emission Tomography | - |
| *CT* | Computed Tomography | - |
| *MRI* | Magnetic Resonance Imaging | - |
| *MRT* | Megavoltage Radiation Therapy | - |
| *IMRT* | Intensity-Modulated Radiation Therapy | - |
| *IGRT* | Image-Guided Radiation Therapy | - |
| *FF* | Flattening Filter | - |
| *MLC* | Multileaf Collimator | - |
| *MCNP* | Monte Carlo N-Particle Transport Code | - |
| *RWD3* | Phantom model | - |
| *PSF* | Phase Space File | - |
| *QA* | Quality Factor | - |

## 1. Introduction

Recently, radiotherapy has been the primary therapy for cancerous tumours in the world and around at least half of the patients with cancer have received this treatment [1- 2]. It is a cytotoxic treatment that can be used for localized solid tumours [3]. It is categorized based on two different methods: brachytherapy and external radiotherapy. In brachytherapy, radioactive sources, directly or using catheters, are sent into or next to the cancerous tumours [4]. It is reported that radiation usually works in the form of seeds, ribbons, or wires. These are sent into the human body and near the cancerous Tumour

**How to cite this article:**
S. Zare Ganjaroodi, M. Fathalizadeh and E. Zarifi, "Probability assessment of photoneutron production of Varian-Clinac ix linear accelerator using Monte Carlo simulation," *International Journal of Reliability, Risk and Safety: Theory and Application*, vol. 7, no. 1, pp. 37-44, 2024, doi: 10.22034/IJRRS.2024.7.1.5.

[5]. External radiotherapy applies a machine out of the body to direct radiation beams at cancer to kill cancerous cells. It is mainly used for breast, head and neck, anal, prostate, bladder, gynaecological, and lung cancer therapy [6]. It should be mentioned that 3-D conformal radiation treatment is typical of external beam radiation therapy. It applies photos from CT, MRI, and PET scans to precisely control the treatment area, a process called simulation [7-8]. Over the last decade, increasing attention has been paid to the use of linear particle accelerators.

A medical linear accelerator is a machine mostly applied in external beam radiation therapy for patients with cancerous tumours. It provides high-energy x-rays or electrons to the areas of the patient's Tumour [8-9]. The mechanism of this equipment firstly was suggested by Gustav Ising in 1924, but the first system used was made by Rolf Widerøe in 1928 [10]. To make these X-rays, medical centres and clinics utilize particle accelerators that direct electrons to tens of millions of electron volts and then collide them into a metallic position to create the X-ray spectrum applied for cancer treatments [11]. It was reported that using LINAC for radiation therapy was started in 1953 on a patient in London, the UK, at the Hammersmith Hospital via an 8 (MV) (a system made by Metropolitan-Vickers and installed in 1952, as the first applied medical linac [12]. It is also called MRT in some references [12]. Figure 1 shows the first usage of this machine on a child named Gordon Isaacs, who was the first patient treated with linear accelerator radiation therapy (in this case, an electron beam) in 1957 in the U.S [13].

In external beam radiotherapy, the gantry surrounds the patient with a radiation source. Moreover, LINAC is placed on the top of the gantry, and a rectangular screen on the right side of the gantry is a cone beam x-ray detector applied to help position a patient before therapy [14-15]. This process is shown in Figure 2 as follows.

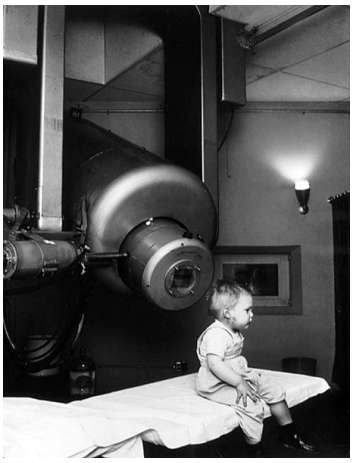

**Figure 1.** The first usage of LINAC

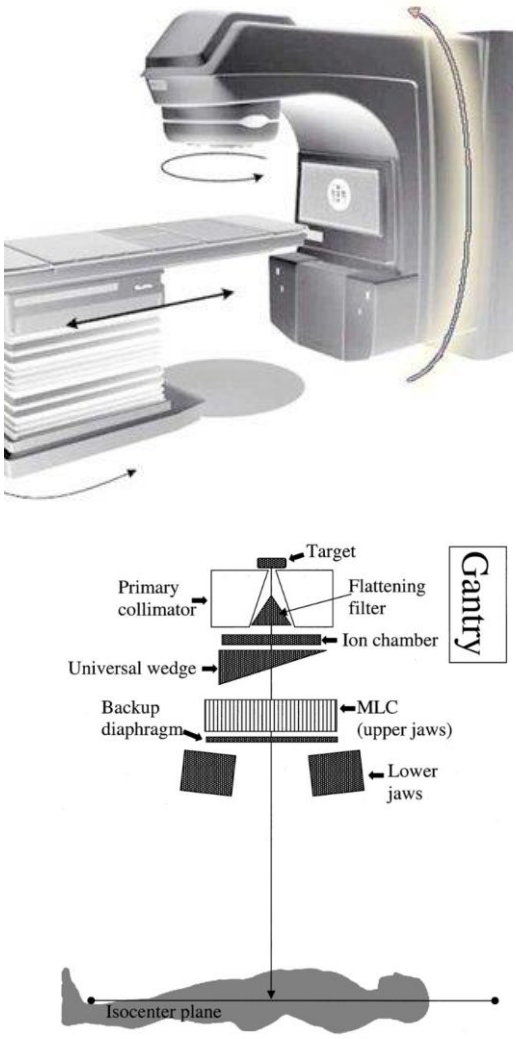


**Figure 2.** The gantry of external beam radiotherapy **[15]**

According to Figure 2, it is protected via a drive stand, which rotates the gantry on a stable horizontal axis as the LINAC revolves around a patient. A klystron in the drive stands behind the gantry and provides radio frequency energy to the LINAC. The LINAC accelerates a pencil-sized beam of electrons horizontally. After leaving the LINAC, the electrons are deflected and focused downward by magnets, causing the electrons to strike the tungsten target. The target stops the electrons, and the sudden deceleration results in bremsstrahlung radiation of X-rays [15].

Today, Varian Medical Systems, Inc. introduced the Clinac iX linear accelerator, Varian's most ergonomic and customizable technology platform for treating cancer with image-guided radiotherapies. Designed to help clinics maximize their technology investment, each Clinac iX is easily installed, customized, configured, and upgraded to support every type of radiotherapy treatment process, from conventional 2D and 3D treatments to the most sophisticated forms of IMRT and IGRT. The Clinac

iX is an ideal platform for dynamic targeting IGRT and beyond. Like its predecessor, the Clinac EX, it is designed to enable therapists to deliver the most sophisticated, complex treatments within a normal treatment appointment timeframe," says Richard Stark, director of Varian's delivery systems product line. "It is a comprehensive, workflow-oriented solution enabling treatment facilities to implement IGRT more quickly and efficiently [16].

Several reports and essays on various technical aspects of the Varian-Clinac ix linear accelerator have been studied in recent years. Li Chen et al. 2009 analysed and compared small-field measurements using different methods and ionization chambers. Results show for the beam size of > or=3 cm * 3 cm, the differences in total scatter factor and collimator scatter factor measurements of the 0.65 cc, 0.13 cc and 0.01 cc ion chambers were within 0.8%, while the differences were much greater for the beam size of less than 3 cm * 3 cm (the maximum difference reached 64%). Also, For the measurement of small fields, the choice of a suitable detector is important due to the lack of lateral electron equilibrium [17]. In 1971, Suresh et al. studied the tissue maximum dose ratio for 8 MeV X-rays. The calculated data have been compared with experimental measurements, and the results are agreed upon [18]. In another study, Mohammad Ashrafinia et al. investigated LINAC Structural Effects on Photoneutron Specified Parameters Using FLUKA code in 2019. This study aimed to evaluate the effect of the physical components of the head, including Flattening Filter (FF) and Multileaf Collimator (MLC), as well as the dependence of therapeutic field size on the photoneutron spectrum, dose, and flux. They found that this paper aimed to evaluate the effect of the physical components of the head, including flattening Filter (FF) and multileaf collimator (MLC), as well as the dependence of therapeutic field size on the photoneutron spectrum, dose, and flux. Photoneutron spectrum analysis indicated that neutrons with the highest relative biological effectiveness were delivered to the phantom surface, and opening the field from 0×0 to 40×40 $cm^2$ shifted the spectrum by 24.545% to the higher energies. The target and the vicinity parts played the most prominent roles in neutron contamination [19]. Andy Ma et al. studied the Monte Carlo study of photoneutron production in the Varian Clinac 2100C linac in 2008, which was published in the Journal of Radioanalytical and Nuclear Chemistry. This work used the general-purpose Monte Carlo code MCNPX to model the Varian Clinac 2100C linac with a 15 MV photon beam. Simulations are carried out for several field sizes commonly encountered in radiotherapy. The results are a basis for further studies on using the Linac as an alternative neutron source in BNCT and radiation protection issues arising from photoneutrons in the treatment room [20]. In 2009, Bryan Bednarz and George Xu worked on the Monte Carlo modelling of a 6 and 18 MV Varian Clinac medical accelerator for in-field and out-of-field dose calculations in the form of a development and validation paper. This paper describes the development and validation of a detailed accelerator model of the Varian Clinac operating at 6 and 18 MV beam energies. Over 100 accelerator components have been defined and integrated using the Monte Carlo code MCNPX. Results showed that the local difference between calculated and measured doses on the percent depth dose curve was less than 2% for all locations. The local difference between calculated and measured doses on the dose profile curve was less than 2% in the plateau region and less than 2 mm in the penumbra region for all locations. In addition, a method for determining neutron contamination in the 18 MV operating model was validated by comparing calculated in-air neutron fluence with reported calculations and measurements. The average difference between calculated and measured neutron fluence was 20% [21]. E. Hedin et al., in 2010, studied the Monte Carlo simulation of linear accelerator Varian Clinac iX. The document aimed to describe how model parameters have been optimized and how the quality of the model has been verified. The parameters adjusted in the model were the energy of the electrons (monoenergetic) incident (normally) on the target as well as the width of the spatial distribution of the electrons (assumed to be Gaussian). Simulated data were compared to measured data visually quantitively by directly comparing the numbers and by statistically weighting the differences in a $chi^2$/NDF analysis [22]. Taha Hachemi et al. studied the PENELOPE simulations and experiments for 6 MV Clinac iX accelerators for standard and small static fields in 2021. They aimed to produce accurate data for use as a gold standard and a valid tool for measurements in reference dosimetry for standard and small static field sizes from $0.5 \times 0.5$ to $10 \times 10$ $cm^2$, which is based on the accuracy of the PSFs as a key quantity [23]. In 2020, Mustapha Assalmi et al. evaluated the computation time efficiency of the multithreaded code (G4Linac-MT) in the dosimetry application, using the high performance of the HPC-Marwan grid to determine with high accuracy the initial parameters of the 6 MV photon beam of Varian CLINAC 2100C [24]. Seiichi_Yamamoto et al. used luminol water for dose distribution measurements of high-energy X-rays from a LINAC. Imaging of the light emitted from luminol water was conducted using a cooled charge-coupled device (CCD) camera during irradiation with 6 MV X-rays from a LINAC to the luminol water. Also, they confirmed that imaging luminol water was promising for dose distribution imaging by correcting the Cherenkov-light component in the images [25].

One of the essential goals of radiation therapy, which has received less attention in previous studies, is to protect healthy tissues from radiation absorption. The neutron produced in Linac has a QA of 20, creating a high equivalent dose in the tissue. In this study, the 18 MV

Varian-Clinac ix is modelled to calculate the photoneutron production in each gantry component. According to the probabilistic structure of the collision of the radiation emitted from the Clinac with healthy tissue and other gantry components, the MCNPX code, which uses the Monte Carlo method based on probabilities, has been performed with high accuracy for modelling.

## 2. Materials and Methods

MCNP is a general and consequential Monte Carlo radiation transport code that tracks many particle types over broad ranges of energies, including photons, neutrons, and electrons. It is ideally suited to the needs of professionals interested in performing radiation shielding and sky shine calculations, detector simulation studies, or dosimetry. The MCNP code does not solve an explicit transport equation but obtains answers by simulating individual particles and recording some tallies of individual particle average behaviour using the Monte Carlo method. Then, the average behaviour of the particles in the physical system is interpreted as the average behaviour of the simulated particles [26-27].

To check the ideal state of shielding, the maximum amount of opening of the two pairs of collimators' jaws is considered, in which a field equal to 40 * 40 $cm^2$ is created. Hence, the accelerator can pass the maximum number of photons in this situation. It should be noted that the primary collimator is fixed in the accelerator, so the field size must be adjusted with the secondary collimator, which itself performs square field calculations by default [28-29]. In other words, the proportions of the openings of the secondary collimator jaws must be determined using the proportions of two nested triangles that intersect at the apex to create a 40 × 40 $cm^2$ field at the phantom surface.

Varian-Clinac ix linear accelerator (Figure 3) can produce photons with energies of 6 MV and 18 MV, but because the safest values must be considered at maximum accelerator energy for shielding, the output energy of 18 MV is selected for modelling. Moreover, the treatment room modelled in this study is rectangular and has an area of 25 m2. This paper modelled the system geometry, radiation source and phantom. The results for 20 million photons in the MCNPX code based on the Monte Carlo method were obtained, and the contribution of each accelerator gantry component in the production of photon neutrons at different energy ranges was calculated using the F4 and F7 tallies. Finally, at different depths of the RDW3 simulated phantom, the amount of absorption neutrons is extracted and benchmarked with the previous reports, which shows an acceptable error of less than 0.5% for the photoneutron values produced in accelerator gantry components and about 4% was obtained for the number of photoneutrons produced in the phantom. The modelling flowchart is presented in Figure 4. A scheme of device simulation via MCNPX code is shown in Figure 5.

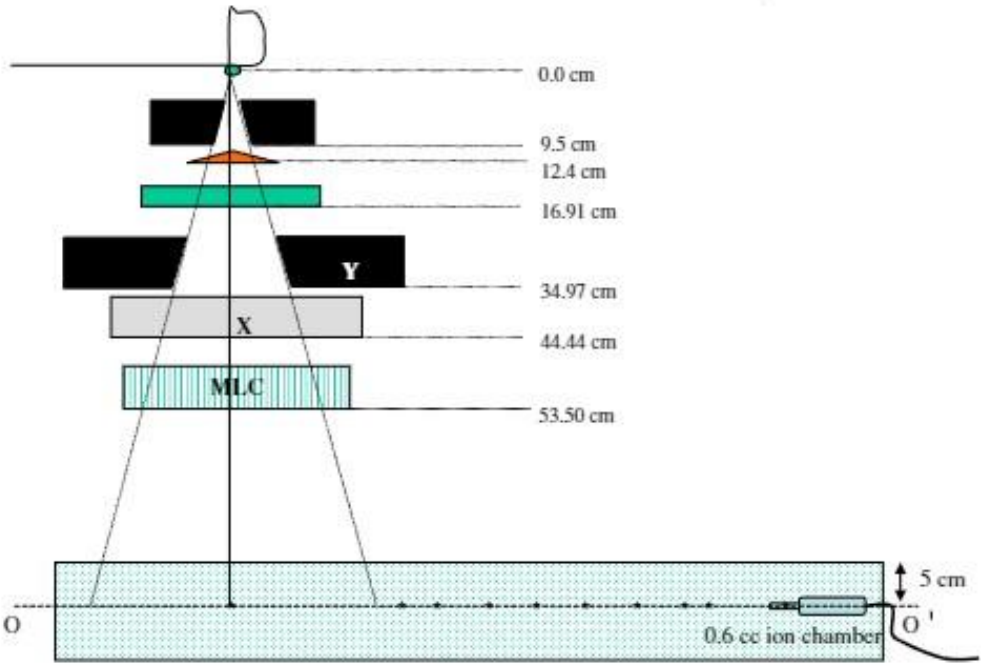


**Figure 3.** Varian-Clinac ix linear accelerator dimensions

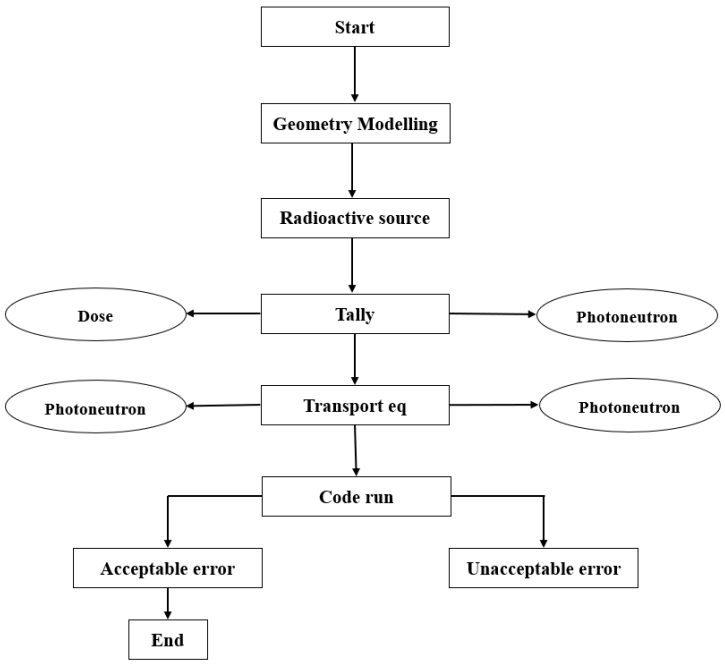


**Figure 4.** Present modelling flowchart

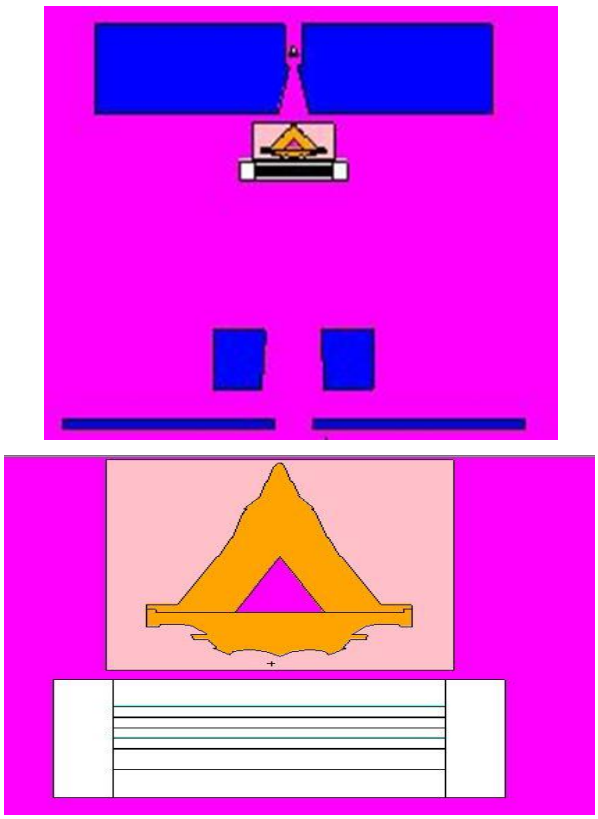

**Figure 5.** Varian-Clinac ix modelling by MCNPX code

# 3. Results and Discussion

In this study, the input of MCNPX code was run for 20 million photons by a supercomputer to calculate the contribution of each accelerator gantry component in the production of photoneutrons at different energy intervals. Also, at different depths of the RDW3 modelled phantom, the amount of absorption neutron dose is calculated. The amounts of photoneutrons produced in different accelerator components per gray of absorbed photon dose are listed in Table 1.

**Table 1.** Amounts of produced photoneutrons in different accelerator components per gray

| Components | Energy Range (MeV) | | | |
|---|---|---|---|---|
| | 0 to 2.50 E -8 | 2.50 E-8 to 7.00 E-7 | 4.00 E-7 to 1.00 | 1.00 to 20.00 |
| | Fluence (neutron/(cm$^2$.Gy$^{-1}$)) | | | |
| Primary collimator | 1.30 E+8 | 9.69 E+8 | 1.00 E+12 | 1.19 E+13 |
| Secondary collimator | 1.53 E+8 | 1.67 E+9 | 2.76 E+11 | 3.99 E+12 |
| Flattening filter | 1.59 E+7 | 3.29 E+7 | 1.52 E+11 | 3.67 E+10 |
| MLC | 1.06 E+7 | 3.29 E+7 | 1.87 E+10 | 1.52 E+11 |
| Target | 0 | 2.23 E+6 | 1.24 E+11 | 3.02 E+6 |
| Phantom | 1.58 E+4 | 2.68 E+4 | 0.61E +11 | 5.81 E+7 |

The results showed that the highest share of photon neutron production was related to the primary collimator, secondary collimator, target, MLC and radiation flattening Filter, respectively. A comparison of results

with some related studies and reports shows good agreement [30-31].

According to the data, it is evident that the volume of each component and the proximity of the components to the radiation source are not related to the amount of photon neutron flux produced in that component. Also, in the target, which is the first source of photon neutron production, the flux of thermal neutrons is zero.

On the other hand, the most significant ratio of photoneutron production in the accelerator is related to primary collimators. Hence, this fact can be used for conservation studies in Varian Clinac ix. In such a manner, the amount of neutron flux produced in the primary collimator can be measured to be considered the safest state for the protection design. Absorption dose values produced in the phantom per gram of absorbed photon dose are illustrated in Table 2. The ratio of each accelerator component in the amount of photoneutrons produced is shown in Figure 6.

**Table 2.** Absorption dose values produced in the phantom per gray of absorbed photon dose

| Energy Range (MeV) | Dose (mSV.Gy$^{-1}$)) |
|---|---|
| 0 – 2.50 E -8 | 1.535 E+8 |
| 2.50 E-8 – 7.00 E-7 | 1.677 E+9 |
| 4.00 E-7 - 1.00 | 2.766 E+11 |
| 1.00 - 20.00 | 3.993 E+12 |

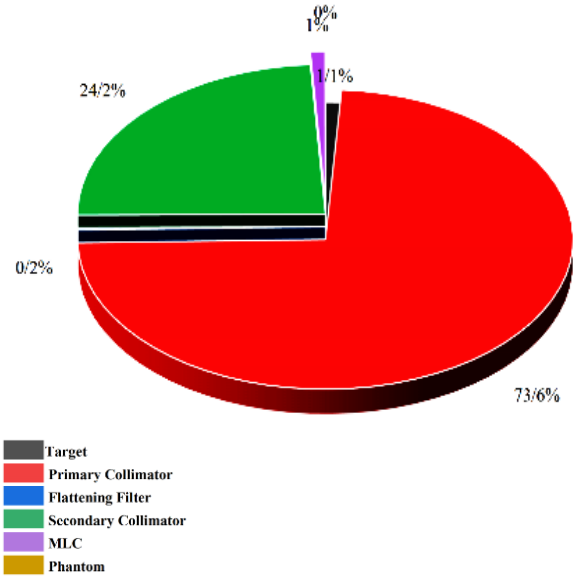


**Figure 6.** The ratio of each accelerator component in the number of photoneutrons produced

## 4. Conclusions

To investigate and prevent the destructive biological effects on the patient's body, neutron dosimetry is very important in the treatment process in the linear accelerator. After modelling the Varian-Clinac ix linear accelerator 18 (MV) using the Monte Carlo modelling by MCNPX code, the contribution of each accelerator gantry component in the production of photoneutrons at different energy intervals was calculated. Also, at different depths of the RDW3 simulated phantom, the amount of absorption neutrons dose was obtained. In this study, the results were calculated for 20 million photons with an energy of 18 (MV) in the MCNPX code, which showed an error of less than half a percent for the photoneutrons produced in the accelerator gantry components and about four percent error for the photoneutrons produced in the phantom. Results showed that the primary and secondary collimators have the most significant ratio in the production of photoneutrons produced among the gantry components per gray of absorbed dose of photons, respectively. Hence, in the shielding studies for the device, the amount of neutron flux produced in the primary collimator can be used as a criterion to be considered the safest state for the shield design. Also, the volume of each component and the proximity of each component to the radiation source have no relationship with the number of photoneutrons produced in that component.

## 5. Conflicts of interest

The authors declared that they have no conflicts of interest in this paper. Also, they declare the following financial interests that represent a conflict of interest in connection with the research works submitted.

## 6. Ethical Consideration

The authors of the article certify that all ethical principles related to research have been completely met.

## 7. References

[1] S. Yani, R. Tursinah, M. F. Rhani, R. C. X. Soh, F. Haryanto, and I. Arif, "Neutron contamination of Varian Clinac iX 10 MV photon beam using Monte Carlo simulation," *Journal of Physics: Conference Series*, vol. 694, no. 1, p. 012020, 2016/03/01 2016, doi: https://iopscience.iop.org/article/10.1088/1742-6596/694/1/012020.

[2] D. E. Citrin, "Recent Developments in Radiotherapy," *New England Journal of Medicine*, vol. 377, no. 11, pp. 1065-1075, 2017, doi: https://www.nejm.org/doi/10.1056/NEJMra1608986.

[3] D. Schaue and W. H. McBride, "Opportunities and challenges of radiotherapy for treating cancer," (in eng), *Nat Rev Clin Oncol*, vol. 12, no. 9, pp. 527-540, Sep 2015, doi: https://doi.org/10.1038/nrclinonc.2015.120.

[4] Y. Yamamoto *et al.*, "Tumour and immune cell dynamics explain the PSA bounce after prostate

cancer brachytherapy," (in eng), *Br J Cancer*, vol. 115, no. 2, pp. 195-202, Jul 12 2016, doi: https://doi.org/10.1038%2Fbjc.2016.171.

[5] I. Kaiserman, I. Anteby, I. Chowers, E. Z. Blumenthal, I. Kliers, and J. Pe'er, "Post-brachytherapy initial tumour regression rate correlates with metastatic spread in posterior uveal melanoma," *British Journal of Ophthalmology*, vol. 88, no. 7, pp. 892-895, 2004, doi: https://doi.org/10.1136%2Fbjo.2003.036285.

[6] U. Veronesi *et al.*, "Intraoperative radiotherapy versus external radiotherapy for early breast cancer (ELIOT): a randomised controlled equivalence trial," *The Lancet Oncology*, vol. 14, no. 13, pp. 1269-1277, 2013, doi: https://doi.org/10.1016/S1470-2045(13)70497-2.

[7] E. Abel *et al.*, "Impact on quality of life of IMRT versus 3-D conformal radiation therapy in head and neck cancer patients: A case control study," *Advances in Radiation Oncology*, vol. 2, no. 3, pp. 346-353, 2017/07/01/ 2017, doi: https://doi.org/10.1016/j.adro.2017.05.002.

[8] S. Chun *et al.*, "Comparison of 3-D conformal and intensity modulated radiation therapy outcomes for locally advanced non-small cell lung cancer in NRG Oncology/RTOG 0617," *International Journal of Radiation Oncology, Biology, Physics*, vol. 93, no. 3, pp. S1-S2, 2015, doi: http://dx.doi.org/10.1016/j.ijrobp.2015.07.010.

[9] R. Krishnan, "Development of electron linear accelerators in SAMEER," in *Proceedings of the seventh DAE-BRNS Indian particle accelerator conference: book of abstracts*, 2015. [Online]. Available: https://inis.iaea.org/search/search.aspx?orig_q=RN:47048430.

[10] R. Wideröe, "Über ein neues Prinzip zur Herstellung hoher Spannungen," *Arbeiten aus dem Elektrotechnischen Institut der Technischen Hochschule Aachen: Band III: 1928*, pp. 157-176, 1929, doi: https://doi.org/10.1007/978-3-662-40440-9_14.

[11] N. Juntong, R. Chimchang, S. Rimjaem, and C. Saisa-ard, "Design of Electron Gun and S-Band Structure for Medical Electron Linear Accelerator," in *7th Int. Particle Accelerator Conf.(IPAC'16), Busan, Korea, May 8-13, 2016*, 2016: JACOW, Geneva, Switzerland, pp. 1930-1932. [Online]. Available: https://accelconf.web.cern.ch/ipac2016/papers/tupoy015.pdf

[12] D. I. Thwaites and J. B. Tuohy, "Back to the future: the history and development of the clinical linear accelerator," *Physics in Medicine & Biology*, vol. 51, no. 13, p. R343, 2006/06/20 2006, doi: https://dx.doi.org/10.1088/0031-9155/51/13/R20.

[13] B. T. Cooper, R. E. Vatner, and H. A. Shih, "Brain Irradiation Paradigms for Childhood Central Nervous System Tumors," *Pituitary Disorders of Childhood: Diagnosis and Clinical Management*, pp. 299-320, 2019, doi: http://dx.doi.org/10.1007/978-3-030-11339-1_16.

[14] D. Hoffman, E. Chung, C. Hess, R. Stern, and S. Benedict, "Characterization and evaluation of an integrated quality monitoring system for online quality assurance of external beam radiation therapy," *Journal of Applied Clinical Medical Physics*, vol. 18, no. 1, pp. 40-48, 2017, doi: https://doi.org/10.1002/acm2.12014.

[15] L. J. Murray and J. Lilley, "Radiotherapy: technical aspects," *Medicine*, vol. 48, no. 2, pp. 79-83, 2020/02/01/ 2020, doi: https://doi.org/10.1016/j.mpmed.2019.11.003.

[16] "Varian Medical Systems, Inc, Varian Medical Systems Introduces Clinac iX™ Line of High-Performance Linear Accelerators for Treating Cancer," *Oncology*, October 2004, [Online], Available: https://www.varian.com/about-varian/newsroom/press-releases/varian-medical-systems-introduces-clinac-ixtm-line-high

[17] L. Chen *et al.*, "Measurements and comparisons for data of small beams of linear accelerators," *Chinese journal of cancer*, vol. 28, no. 3, pp. 272-276, 2009. [Online]. Available: https://pubmed.ncbi.nlm.nih.gov/19619452/.

[18] S. K. Agarwal, R. V. SCHEELE, and J. WAKLEY, "Tissue maximum-dose ratio (Tmr) for 8 MV X rays," *American Journal of Roentgenology*, vol. 112, no. 4, pp. 797-802, 1971, doi: https://doi.org/10.2214/ajr.112.4.797.

[19] M. Ashrafinia, A. Hadadi, D. Sardari, and E. Saeedzadeh, "Investigation of LINAC structural effects on photoneutron specified parameters using FLUKA code," *Iranian Journal of Medical Physics*, vol. 17, no. 1, pp. 7-14, 2020, doi: https://doi.org/10.22038/ijmp.2019.37678.1481.

[20] A. Ma, J. Awotwi-Pratt, A. Alghamdi, A. Alfuraih, and N. Spyrou, "Monte Carlo study of photoneutron production in the Varian Clinac 2100C linac," *Journal of Radioanalytical and Nuclear Chemistry*, vol. 276, no. 1, pp. 119-123, 2008, doi: http://dx.doi.org/10.1007/s10967-007-0419-3.

[21] B. Bednarz and X. G. Xu, "Monte Carlo modeling of a 6 and 18 MV Varian Clinac medical accelerator for in-field and out-of-field dose calculations: development and validation," *Physics in Medicine & Biology*, vol. 54, no. 4, p. N43, 2009, doi: https://doi.org/10.1088%2F0031-9155%2F54%2F4%2FN01.

[22] E. Hedin, A. Bäck, J. Swanpalmer, and R. Chakarova, "Monte Carlo simulation of linear accelerator Varian Clinac iX," *Report MFT-Radfys*, vol. 1, 2010. [Online]. Available: https://www-

nds.iaea.org/phsp/photon1/VarianClinaciX_6MV_PHSPdoc_Gothenburg.pdf.

[23] T. Hachemi and S. Khoudri, "PENELOPE simulations and experiment for 6 MV clinac iX accelerator for standard and small static fields," *Applied Radiation and Isotopes*, vol. 174, p. 109749, 2021, doi: https://doi.org/10.1016/j.apradiso.2021.109749.

[24] M. Assalmi and N. Mansour, "Validation of Monte carlo Geant4 multithreading code for a 6 MV photon beam of varian linac on the grid computing," *Reports of Practical Oncology and Radiotherapy*, vol. 25, no. 6, pp. 1001-1010, 2020, doi: https://doi.org/10.1016/j.rpor.2020.09.011.

[25] S. Yamamoto, K. Yamada, T. Yabe, Y. Hirano, and J. Kataoka, "Dose distribution measurements using luminol water during irradiation of high-energy X-rays from medical linear accelerators (LINAC)," *Radiation Physics and Chemistry*, vol. 208, p. 110895, 2023, doi: https://doi.org/10.1016/j.radphyschem.2023.110895.

[26] D. B. Pelowitz, "MCNPXTM user's manual," *Los Alamos National Laboratory, Los Alamos,* vol. 5, p. 369, 2005. [Online]. Available: http://prof.khuisf.ac.ir/images/Uploaded_files/1354176297.2.6.0_Users_Manual%5b6730939%5d.PDF.

[27] B. Liu, X. Lv, W. Zhao, K. Wang, J. Tu, and X. Ouyang, "The comparison of MCNP perturbation technique with MCNP difference method in critical calculation," *Nuclear engineering and design*, vol. 240, no. 8, pp. 2005-2010, 2010, doi: https://doi.org/10.1016/j.nucengdes.2010.04.022.

[28] X. Wang, C. Esquivel, E. Nes, C. Shi, N. Papanikolaou, and M. Charlton, "The neutron dose equivalent evaluation and shielding at the maze entrance of a Varian Clinac 23EX treatment room," *Medical physics*, vol. 38, no. 3, pp. 1141-1149, 2011, doi: https://doi.org/10.1118/1.3533713.

[29] Khan, F.M. and J.P. Gibbons, Khan's the physics of radiation therapy, *Journal of medical physics*, 2014: Lippincott Williams & Wilkins, DOI: https://doi.org/10.4103%2Fjmp.JMP_17_20

[30] H. A. Nedaie *et al.*, "Neutron dose measurements of Varian and Elekta linacs by TLD600 and TLD700 dosimeters and comparison with MCNP calculations," *Journal of Medical Physics*, vol. 39, no. 1, pp. 10-17, 2014, doi: https://doi.org/10.4103/0971-6203.125476.

[31] H. Yücel, İ. Çobanbaş, A. Kolbaşı, A. Ö. Yüksel, and V. Kaya, "Measurement of photo-neutron dose from an 18-MV medical linac using a foil activation method in view of radiation protection of patients," *Nuclear engineering and technology*, vol. 48, no. 2, pp. 525-532, 2016, doi: https://doi.org/10.1016/j.net.2015.11.003.